Dijet imbalance measurements in Au + Au and pp collisions at $\sqrt{s_{NN}} = 200$ GeV at STAR

L. Adamczyk,[1] J. K. Adkins,[19] G. Agakishiev,[17] M. M. Aggarwal,[31] Z. Ahammed,[50] I. Alekseev,[15,26] D. M. Anderson,[42] R. Aoyama,[3] A. Aparin,[17] D. Arkhipkin,[3] E. C. Aschenauer,[3] M. U. Ashraf,[45] A. Attri,[31] G. S. Averichev,[17] X. Bai,[7] V. Bairathi,[27] R. Bellwied,[44] A. Bhasin,[16] A. K. Bhati,[31] P. Bhattarai,[43] J. Bielcik,[10] J. Bielcikova,[11] L. C. Bland,[3] I. G. Bordyuzhin,[15] J. Bouchet,[18] J. D. Brandenburg,[36] A. V. Brandin,[26] D. Brown,[23] I. Bunzarov,[17] J. Butterworth,[36] H. Caines,[54] M. Calderón de la Barca Sánchez,[5] J. M. Campbell,[29] D. Cebra,[5] I. Chakaberia,[3] P. Chaloupka,[10] Z. Chang,[42] A. Chatterjee,[50] S. Chattopadhyay,[50] J. H. Chen,[39] X. Chen,[21] J. Cheng,[45] M. Cherney,[9] W. Christie,[3] G. Contin,[22] H. J. Crawford,[4] S. Das,[13] L. C. De Silva,[9] R. R. Debbe,[3] T. G. Dedovich,[17] J. Deng,[38] A. A. Derevschikov,[33] L. Didenko,[3] C. Dilks,[32] X. Dong,[22] J. L. Drachenberg,[20] J. E. Draper,[5] C. M. Du,[21] L. E. Dunkelberger,[6] J. C. Dunlop,[3] L. G. Efimov,[17] N. Elsey,[52] J. Engelage,[4] G. Eppley,[36] R. Esha,[6] S. Esumi,[46] O. Evdokimov,[8] J. Ewigleben,[23] O. Eyser,[3] R. Fatemi,[19] S. Fazio,[3] P. Federic,[11] J. Fedorisin,[17] Z. Feng,[7] P. Filip,[17] E. Finch,[47] Y. Fisyak,[3] C. E. Flores,[5] L. Fulek,[1] C. A. Gagliardi,[42] D. Garand,[34] F. Geurts,[36] A. Gibson,[49] M. Girard,[51] L. Greiner,[22] D. Grosnick,[49] D. S. Gunarathne,[41] Y. Guo,[37] A. Gupta,[16] S. Gupta,[16] W. Guryn,[3] A. I. Hamad,[18] A. Hamed,[42] R. Haque,[27] J. W. Harris,[54] L. He,[34] S. Heppelmann,[32] S. Heppelmann,[5] A. Hirsch,[34] G. W. Hoffmann,[43] S. Horvat,[54] X. Huang,[45] B. Huang,[8] H. Z. Huang,[6] T. Huang,[28] P. Huck,[7] T. J. Humanic,[29] G. Igo,[6] W. W. Jacobs,[14] A. Jentsch,[43] J. Jia,[3,40] K. Jiang,[37] S. Jowzaee,[52] E. G. Judd,[4] S. Kabana,[18] D. Kalinkin,[14] K. Kang,[45] K. Kauder,[52] H. W. Ke,[3] D. Keane,[18] A. Kechechyan,[17] Z. Khan,[8] D. P. Kikoła,[51] I. Kisel,[12] A. Kisiel,[51] L. Kochenda,[26] D. D. Koetke,[49] L. K. Kosarzewski,[51] A. F. Kraishan,[41] P. Kravtsov,[26] K. Krueger,[2] L. Kumar,[31] M. A. C. Lamont,[3] J. M. Landgraf,[3] K. D. Landry,[6] J. Lauret,[3] A. Lebedev,[3] R. Lednicky,[17] J. H. Lee,[3] W. Li,[39] X. Li,[41] X. Li,[37] Y. Li,[45] C. Li,[37] T. Lin,[14] M. A. Lisa,[29] Y. Liu,[42] F. Liu,[7] T. Ljubicic,[3] W. J. Llope,[52] M. Lomnitz,[18] R. S. Longacre,[3] X. Luo,[7] S. Luo,[8] G. L. Ma,[39] L. Ma,[39] R. Ma,[3] Y. G. Ma,[39] N. Magdy,[40] R. Majka,[54] A. Manion,[22] S. Margetis,[18] C. Markert,[43] H. S. Matis,[22] D. McDonald,[44] S. McKinzie,[22] K. Meehan,[5] J. C. Mei,[38] Z. W. Miller,[8] N. G. Minaev,[33] S. Mioduszewski,[42] D. Mishra,[27] B. Mohanty,[27] M. M. Mondal,[42] D. A. Morozov,[33] M. K. Mustafa,[22] Md. Nasim,[6] T. K. Nayak,[50] G. Nigmatkulov,[26] T. Niida,[52] L. V. Nogach,[33] T. Nonaka,[46] J. Novak,[25] S. B. Nurushev,[33] G. Odyniec,[22] A. Ogawa,[3] K. Oh,[35] V. A. Okorokov,[26] D. Olvitt, Jr.,[41] B. S. Page,[3] R. Pak,[3] Y. X. Pan,[6] Y. Pandit,[8] Y. Panebratsev,[17] B. Pawlik,[30] H. Pei,[7] C. Perkins,[4] P. Pile,[3] J. Pluta,[51] K. Poniatowska,[51] J. Porter,[22] M. Posik,[41] A. M. Poskanzer,[22] N. K. Pruthi,[31] M. Przybycien,[1] J. Putschke,[52] H. Qiu,[34] A. Quintero,[41] S. Ramachandran,[19] R. L. Ray,[43] R. Reed,[23,55] M. J. Rehbein,[9] H. G. Ritter,[22] J. B. Roberts,[36] O. V. Rogachevskiy,[17] J. L. Romero,[5] J. D. Roth,[9] L. Ruan,[3] J. Rusnak,[11] O. Rusnakova,[10] N. R. Sahoo,[42] P. K. Sahu,[13] I. Sakrejda,[22] S. Salur,[22] J. Sandweiss,[54] J. Schambach,[43] R. P. Scharenberg,[34] A. M. Schmah,[22] W. B. Schmidke,[3] N. Schmitz,[24] J. Seger,[9] P. Seyboth,[24] N. Shah,[39] E. Shahaliev,[17] P. V. Shanmuganathan,[23] M. Shao,[37] M. K. Sharma,[16] A. Sharma,[16] B. Sharma,[31] W. Q. Shen,[39] S. S. Shi,[7] Z. Shi,[22] Q. Y. Shou,[39] E. P. Sichtermann,[22] R. Sikora,[1] M. Simko,[11] S. Singha,[18] M. J. Skoby,[14] D. Smirnov,[3] N. Smirnov,[54] W. Solyst,[14] L. Song,[44] P. Sorensen,[3] H. M. Spinka,[2] B. Srivastava,[34] T. D. S. Stanislaus,[49] M. Stepanov,[34] R. Stock,[12] M. Strikhanov,[26] B. Stringfellow,[34] T. Sugiura,[46] M. Sumbera,[11] B. Summa,[32] X. M. Sun,[7] Z. Sun,[21] Y. Sun,[37] B. Surrow,[41] D. N. Svirida,[15] Z. Tang,[37] A. H. Tang,[3] T. Tarnowsky,[25] A. Tawfik,[53] J. Thäder,[22] J. H. Thomas,[22] A. R. Timmins,[44] D. Tlusty,[36] T. Todoroki,[3] M. Tokarev,[17] S. Trentalange,[6] R. E. Tribble,[42] P. Tribedy,[3] S. K. Tripathy,[56] O. D. Tsai,[6] T. Ullrich,[3] D. G. Underwood,[2] I. Upsal,[29] G. Van Buren,[3] G. van Nieuwenhuizen,[3] A. N. Vasiliev,[33] R. Vertesi,[11] F. Videbæk,[3] S. Vokal,[17] S. A. Voloshin,[52] A. Vossen,[14] F. Wang,[34] J. S. Wang,[21] G. Wang,[6] Y. Wang,[45] Y. Wang,[7] G. Webb,[3] J. C. Webb,[3] L. Wen,[6] G. D. Westfall,[25] H. Wieman,[22] S. W. Wissink,[14] R. Witt,[48] Y. Wu,[18] Z. G. Xiao,[45] G. Xie,[37] W. Xie,[34] K. Xin,[36] Q. H. Xu,[38] H. Xu,[21] Y. F. Xu,[39] Z. Xu,[3] J. Xu,[7] N. Xu,[22] S. Yang,[37] Q. Yang,[37] Y. Yang,[57] C. Yang,[37] Y. Yang,[7] Y. Yang,[21] Z. Ye,[8] Z. Ye,[8] L. Yi,[54] K. Yip,[3] I.-K. Yoo,[35] N. Yu,[7] H. Zbroszczyk,[51] W. Zha,[37] X. P. Zhang,[45] J. Zhang,[21] J. Zhang,[38] Z. Zhang,[39] S. Zhang,[37] J. B. Zhang,[7] Y. Zhang,[37] S. Zhang,[39] J. Zhao,[34] C. Zhong,[39] L. Zhou,[37] X. Zhu,[45] Y. Zoulkarneeva,[17] and M. Zyzak[12]

(STAR Collaboration)

[1]AGH University of Science and Technology, FPACS, Cracow 30-059, Poland
[2]Argonne National Laboratory, Argonne, Illinois 60439
[3]Brookhaven National Laboratory, Upton, New York 11973
[4]University of California, Berkeley, California 94720

[5]University of California, Davis, California 95616
[6]University of California, Los Angeles, California 90095
[7]Central China Normal University, Wuhan, Hubei 430079
[8]University of Illinois at Chicago, Chicago, Illinois 60607
[9]Creighton University, Omaha, Nebraska 68178
[10]Czech Technical University in Prague, FNSPE, Prague 115 19, Czech Republic
[11]Nuclear Physics Institute AS CR, 250 68 Prague, Czech Republic
[12]Frankfurt Institute for Advanced Studies FIAS, Frankfurt 60438, Germany
[13]Institute of Physics, Bhubaneswar 751005, India
[14]Indiana University, Bloomington, Indiana 47408
[15]Alikhanov Institute for Theoretical and Experimental Physics, Moscow 117218, Russia
[16]University of Jammu, Jammu 180001, India
[17]Joint Institute for Nuclear Research, Dubna 141 980, Russia
[18]Kent State University, Kent, Ohio 44242
[19]University of Kentucky, Lexington, Kentucky 40506-0055
[20]Lamar University, Physics Department, Beaumont, Texas 77710
[21]Institute of Modern Physics, Chinese Academy of Sciences, Lanzhou, Gansu 730000
[22]Lawrence Berkeley National Laboratory, Berkeley, California 94720
[23]Lehigh University, Bethlehem, Pennsylvania 18015
[24]Max-Planck-Institut fur Physik, Munich 80805, Germany
[25]Michigan State University, East Lansing, Michigan 48824
[26]National Research Nuclear University MEPhI, Moscow 115409, Russia
[27]National Institute of Science Education and Research, Bhubaneswar 751005, India
[28]National Cheng Kung University, Tainan 70101
[29]The Ohio State University, Columbus, Ohio 43210
[30]Institute of Nuclear Physics PAN, Cracow 31-342, Poland
[31]Panjab University, Chandigarh 160014, India
[32]Pennsylvania State University, University Park, Pennsylvania 16802
[33]Institute of High Energy Physics, Protvino 142281, Russia
[34]Purdue University, West Lafayette, Indiana 47907
[35]Pusan National University, Pusan 46241, Korea
[36]Rice University, Houston, Texas 77251
[37]University of Science and Technology of China, Hefei, Anhui 230026
[38]Shandong University, Jinan, Shandong 250100
[39]Shanghai Institute of Applied Physics, Chinese Academy of Sciences, Shanghai 201800
[40]State University Of New York, Stony Brook, New York 11794
[41]Temple University, Philadelphia, Pennsylvania 19122
[42]Texas A&M University, College Station, Texas 77843
[43]University of Texas, Austin, Texas 78712
[44]University of Houston, Houston, Texas 77204
[45]Tsinghua University, Beijing 100084
[46]University of Tsukuba, Tsukuba, Ibaraki 305-8571, Japan
[47]Southern Connecticut State University, New Haven, Connecticut 06515
[48]United States Naval Academy, Annapolis, Maryland 21402
[49]Valparaiso University, Valparaiso, Indiana 46383
[50]Variable Energy Cyclotron Centre, Kolkata 700064, India
[51]Warsaw University of Technology, Warsaw 00-661, Poland
[52]Wayne State University, Detroit, Michigan 48201
[53]World Laboratory for Cosmology and Particle Physics (WLCAPP), Cairo 11571, Egypt
[54]Yale University, New Haven, Connecticut 06520
[55]Lehigh University, Bethlehem, Pennsylvnia 18015
[56]Institute of Physics, Bhubaneswar 751005, India
[57]National Cheng Kung University, Tainan 70101

We report the first dijet transverse momentum asymmetry measurements from Au + Au and pp
collisions at RHIC. The two highest-energy back-to-back jets reconstructed from fragments with transverse
momenta above 2 GeV/c display a significantly higher momentum imbalance in heavy-ion collisions than
in the pp reference. When reexamined with correlated soft particles included, we observe that these dijets

then exhibit a unique new feature—momentum balance is restored to that observed in pp for a jet resolution
parameter of $R = 0.4$, while rebalancing is not attained with a smaller value of $R = 0.2$.

High-energy collisions of large nuclei at the Relativistic
Heavy Ion Collider (RHIC) at Brookhaven National
Laboratory exceed the energy density at which a strongly
coupled medium of deconfined quarks and gluons, the quark
gluon plasma (QGP), is expected to form [1]. Partons with
large transverse momentum ($p_T \gg \Lambda_{QCD}$) resulting from
hard scatterings provide "hard probes" that allow for the
unique opportunity to explore the QGP tomographically.
Such scatterings occur promptly ($\sim 1/p_T$) in the initial
stages of the collision, and can thus probe the evolution
of the medium. The scattered partons separate and fragment
into back-to-back clusters of collimated hadrons known as
jets. Jet p_T distributions in proton-proton (pp) collisions at
RHIC are well described by perturbative quantum chromo-
dynamics (pQCD) and can be used as a calibrated reference
for studies of medium-induced jet modifications [2].

Production of high-p_T hadrons, serving as a jet proxy,
was first found to be highly suppressed at RHIC in single-
particle measurements compared to scaled pp collisions [3].
Moreover, particle yields on the recoil side of high-p_T
triggered dihadron correlations exhibited a shift from high
to low energy [4]. These observations established the
energy dissipation of fast-moving partons as a key signature
of a dense partonic medium, known as the jet quenching
effect [5,6]. Most theoretical explanations of light quark and
gluon jet quenching in heavy-ion collisions, while differing
in details, identify pQCD-type radiative energy loss (gluon
bremsstrahlung) as the dominant mechanism. Inherent to
these frameworks is the qualitative feature that the jet
structure is softened and broadened with respect to vacuum
expectations [5–8]. Advances in jet-finding techniques [9],
and the proliferation of high-p_T jets at the higher energies
accessible at the Large Hadron Collider (LHC) have made it
possible with a higher center-of-mass energy per nucleon
pair to study fully reconstructed jets in heavy-ion collisions
for the first time [10–12]. Inclusive jet spectra in the most
central (head-on) lead-lead (Pb + Pb) collisions at a center-
of-mass energy per nucleon pair of $\sqrt{s_{NN}} = 2.76$ TeV were
found to be clearly suppressed when compared to scaled pp
or scaled peripheral (glancing) Pb + Pb collisions at the
same collision energy. This suppression occurred independ-
ently of jet p_T for jets with $p_T \sim 40$–210 GeV/c, and even
for jets reconstructed with a resolution parameter as large as
$R = 0.5$ (while the exact meaning of R is algorithm specific,
for the anti-k_T algorithm used throughout this Letter, it
typically corresponds to roughly circular clusters of radius R
in $\Delta R = \sqrt{\Delta\phi^2 + \Delta\eta^2}$ where $\Delta\phi$ is the relative azimuthal
angle and $\Delta\eta$ the relative pseudorapidity).

Recently, analyses of dijet pairs revealed a striking
energy imbalance for highly energetic back-to-back jet
production [11,13]. The reported imbalance observable is
defined as

$$A_J \equiv (p_{T,\text{lead}} - p_{T,\text{sublead}})/(p_{T,\text{lead}} + p_{T,\text{sublead}}) \quad (1)$$

where $p_{T,\text{lead}}$ and $p_{T,\text{sublead}}$ are the transverse momenta
of the leading and subleading (highest and second-highest
p_T) jet, respectively, in the dijets that are required to be
approximately back to back. In this observable, detector
effects in the determination of jet p_T affect numerator and
denominator in a similar manner and thus cancel out to first
order. It is therefore less sensitive to effects of the under-
lying event than inclusive measurements and other dijet
observables. Furthermore, when dijets with large energy
imbalance were examined at the LHC, much of the *lost
energy* of these jets seemed to reemerge as low momentum
particles emitted at large angles (more than 0.8 sr away)
with respect to the dijet axis [12,14,15].

By contrast, at RHIC energies, measurements based on
correlations of hadrons with leading reconstructed jets or
nondecay (direct) photons indicate that the lost energy
remains much closer to the jet axis [16,17], suggesting only
a moderate broadening of the jet structure for all but the
softest constituents. The difference between the RHIC and
LHC energy results could be due to a number of different
reasons; both the details of the experimental analyses and
the mean parton kinematics being probed at the two
facilities differ significantly. In addition, the LHC results
specifically focus on dijets with a large energy imbalance
on an individual event-by-event basis, whereas published
RHIC measurements based on statistical correlations
require treatment of an ensemble-based background.

In this Letter, we present the first dijet imbalance
measurement in central gold-gold (Au + Au) collisions
at RHIC, thus allowing a more direct comparison to jet
quenching measurements at the LHC. The data used in
this analysis were collected by the STAR detector in pp
and Au + Au collisions at $\sqrt{s_{NN}} = 200$ GeV in 2006 and
2007, respectively. Charged tracks are reconstructed
with the time projection chamber (TPC) [18]. The trans-
verse energy (E_T) of neutral hadrons is included by
measuring the energy deposited in the barrel electromag-
netic calorimeter (BEMC) [19], which has a tower size of
0.05×0.05 in azimuth ϕ and pseudorapidity η. To avoid
double-counting, the energy deposited by charged hadrons
in the BEMC is accounted for by full hadronic correction,
in which the transverse momentum of any charged track
that extrapolates to a tower is subtracted from the trans-

energy of that tower. Tower energies are set to zero if they would otherwise become negative via this correction. While full hadronic correction is an overly conservative way to avoid double-counting energy from charged tracks, it has been found to be the most robust approach [20]. All measurements in this Letter were also repeated as a cross-check using the opposite extreme, subtracting only the minimum ionizing particle energy, and all physics conclusions were unaffected. Both the TPC and the BEMC uniformly cover the full azimuth and a pseudorapidity range of $|\eta| < 1$. Events were selected by an online high tower (HT) trigger, which required an uncorrected $E_T > 5.4$ GeV in at least one BEMC tower. In Au + Au collisions, only the most central 20% of the events are analyzed, where event centrality is a measure of the overlap of the colliding nuclei, determined by the raw charged particle multiplicity in the TPC within $|\eta| < 0.5$. Events are restricted to have a primary vertex position along the beam axis of $|v_z| < 30$ cm. Tracks are required to have more than 52% of available points measured in the TPC (up to 45), and a minimum of 20, a distance of closest approach (DCA) to the collision vertex of less than 1 cm, and pseudorapidity within $|\eta| < 1$.

Jets are reconstructed from charged tracks measured in the TPC and neutral particle information recorded by the BEMC, using the anti-k_T algorithm from the FASTJET package [9,21] with resolution parameters $R = 0.4$ and 0.2. The reconstructed jet axes are required to be within $|\eta| < 1 - R$ to avoid partially reconstructed jets at the edge of the acceptance. In this analysis, the initial definition of the dijet pair considers only tracks and towers with $p_T > 2$ GeV/c in the jet reconstruction. This is done to minimize the effects of background fluctuations and combinatorial jets not originating from an initial hard scatter, and to make an average background energy subtraction unnecessary. We will refer to this selection as (di)jets with "hard cores," as most of their energy is carried by just a few high-p_T constituents. The event-by-event background energy density ρ is determined as the median of $p_T^{\mathrm{jet,rec}}/A^{\mathrm{jet}}$ of all but the two leading jets, using the k_T algorithm with the same resolution parameter R as in the nominal jet reconstruction [9]. The area A^{jet} of jets is also found with the FASTJET package (using active ghost particles). At RHIC energies, the median background energy density $\langle\rho\rangle$ when only particles with $p_T > 2$ GeV/c are considered is 0. Hence no event-by-event ρ subtraction is applied for these "hard-core" jets. The small residual influence of background fluctuations is captured by embedding the pp reference hard-core jets into an Au + Au event (after reconstruction). When, later in the analysis, the constituent cut is lowered, ρ is recalculated event-by-event and the corrected jet $p_T = p_T^{\mathrm{jet,rec}} - \rho A^{\mathrm{jet}}$ is used, discarding jets with $p_T < 0$.

The dijet imbalance A_J is initially calculated in Au + Au HT events for leading and subleading jets fulfilling the following requirements: (1) $p_{T,\mathrm{lead}} > 20$ GeV/c and

$p_{T,\mathrm{sublead}} > 10$ GeV/c, (2) $|\phi_{\mathrm{lead}} - \phi_{\mathrm{sublead}} - \pi| < 0.4$ (back-to-back). In this Letter, jet energies are not corrected back to the original parton energies apart from the correction for relative reconstruction efficiency differences between Au + Au and pp described below. In order to make meaningful quantitative comparisons between the dijet imbalance measured in Au + Au to that in $p + p$, it is however necessary to compare jets which have similar initial parton energies in the two collision systems, and to take the remaining effect of background fluctuations into account. The uncertainty on the absolute jet energy scale is 5%, partially cancelling out in A_J. A detailed discussion of jet energy scale uncertainties and background fluctuations can be found in the Supplemental Material [22] which includes Refs. [23–29]. It was shown in [16] that Au + Au HT leading jets are similar to pp HT leading jets embedded in an Au + Au background. A dijet imbalance reference data set is therefore constructed in this analysis via embedding pp HT events into Au + Au minimum bias (i.e., without a high tower trigger) events with a 0%–20% centrality requirement identical to the HT data (pp HT $\oplus$ Au + Au MB). The heavy ion background has the potential to bias an online high tower trigger toward a higher population of low-energy jets that would not be accounted for by the embedding. In a previous study, this effect was conservatively accounted for with a small systematic uncertainty [16]. The relatively high leading jet requirement and the robustness of the observable in this analysis further reduce a potential influence of such a bias. A cross-check with a higher off-line trigger requirement did not show any effect beyond statistics, and we therefore do not assign a systematic uncertainty.

The performance of the TPC and BEMC can vary in different collision systems and over time. The relative TPC tracking efficiency in Au + Au is ca. 90% $\pm$ 7% that of pp [16], and this difference is accounted for in the pp HT $\oplus$ Au + Au MB during embedding by randomly rejecting charged pp tracks with a probability given by this efficiency difference. The uncertainty on this correction is the largest contributor to systematic uncertainty, and it is assessed by repeating the measurement with the respective minimum and maximum efficiency. The tower efficiency in Au + Au collisions relative to pp collisions is 98% $\pm$ 2% [16], and its contribution to systematic uncertainties is negligible compared to the respective TPC uncertainty. The systematics due to the relative tower energy scale uncertainty (2%) are again assessed via the embedding procedure by increasing or decreasing the E_T of all pp towers by 2%. Only the differences between Au + Au and embedded pp are discussed in this Letter, so no absolute uncertainty on Au + Au is explored. The two variations above constitute the systematics, and their quadrature sum is shown in colored shaded boxes in all figures.

In Fig. 1 the A_J distribution from central Au + Au collisions for anti-k_T jets with $R = 0.4$ (solid red circles)

is compared to the *pp* HT embedding reference (*pp* HT ⊕ Au + Au MB, open circles) for a jet constituent-p_T cut of $p_T^{Cut} > 2$ GeV/c. Dijets in central Au + Au collisions are significantly more imbalanced than the corresponding *pp* dijets. To further quantify this difference the *p* value for the hypothesis that the two histograms represent identical distributions was calculated with a Kolmogorov-Smirnov test on the unbinned data [30], i.e., including only the statistical uncertainties. For an estimate of systematic effects we quote the range of minimal and maximal values obtained during efficiency and tower energy scale variations. The calculated *p* value $< 1 \times 10^{-8}$ $(4 \times 10^{-10}$–$1 \times 10^{-6})$ supports the hypothesis that the Au + Au and *pp* HT ⊕ Au + Au data are not drawn from the same parent A_J distributions.

In order to assess if the energy imbalance can be restored for these dijets by including the jet constituents below 2 GeV/c in transverse momentum, the jet-finder was run again on the same events, but with a lower constituent p_T cut of $p_T^{Cut} > 0.2$ GeV/c. The dijet imbalance A_J was then recalculated for jet pairs geometrically matched to the original hard core dijets. For this matching, the highest p_T jet within $\Delta R = \sqrt{\Delta\phi^2 + \Delta\eta^2} < R$ of the hard core jet was chosen. This matching has better than 99% efficiency. To account for the significant low-p_T background, this recalculation used background-corrected jet $p_T = p_T^{jet,rec} - \rho A^{jet}$. In the central data considered here, ρ is a broad distribution with an average value of about 57 (GeV/c)/sr. The reference *pp* HT ⊕ Au + Au MB embedding distribution was recalculated in the same manner. For matched jets, the role of leading and subleading jets is not enforced again, so A_J can now become negative; all figures include a dashed line at 0 to guide the eye.

In Fig. 1 the matched dijet imbalance measured for a low constituent p_T^{Cut} in central Au + Au collisions (solid black squares) is compared to the new *pp* HT ⊕ Au + Au MB embedding reference (open squares). Remarkably, the A_J distribution in Au + Au now reproduces the *pp* data within uncertainties; the *p* value between these two distributions is 0.4 (0.2–0.6). This observation suggests that the jet energy balance can be restored to the level of *pp* in central Au + Au HT events for this class of dijets if low p_T constituents are included within an anti-k_T jet of resolution parameter (radius) $R = 0.4$.

The tremendous increase in background fluctuations below 2 GeV/c could lead to an artificial dijet energy balance unrelated to potential modifications in the jet fragmentation. In the limit of infinitely high background fluctuations, the correlated signal could be washed out to be indistinguishable. To estimate the magnitude of this effect, we employed two different null hypothesis procedures. First, we embedded the Au + Au HT dijets reconstructed with $p_T^{Cut} > 2$ GeV/c (closed red markers in Fig. 1) into
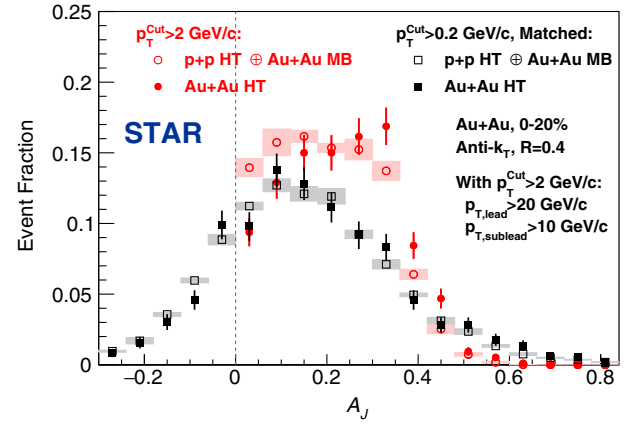

FIG. 1.   Normalized A_J distributions for Au + Au HT data (filled symbols) and *pp* HT ⊕ Au + Au MB (open symbols). The red circles are for jets found using only constituents with $p_T^{Cut} > 2$ GeV/c and the black squares for matched jets found using constituents with $p_T^{Cut} > 0.2$ GeV/c. In all cases $R = 0.4$. Stat. errors may be smaller than symbol size for *pp* HT ⊕ Au + Au MB.

Au + Au MB events with a low constituent $p_T^{Cut} > 0.2$ GeV/c, reperformed the jet finding and matching and recalculated A_J. This procedure explicitly disallows for any balance restoration via correlated signal jet constituents since the jet is embedded into a different random event. We refer to this method as the random cone (RC) technique. In the second method, in order to account for potential nonjet correlations within the event, we embed the same dijet pairs as in the RC method into a different Au + Au HT event with a found dijet pair, at the same azimuth position but randomly off-set in pseudorapidity by at least $2 \times R$. This "eta cone" method (EC) preserves potential background effects due to azimuthal correlations of the underlying event with the jet while also excluding any potential jetlike correlation below 2 GeV/c. Both of these methods are compared to the measured matched A_J distribution with low p_T^{Cut} in Fig. 2. We conclude that background fluctuations do smear the A_J signal significantly with an overall effect toward balancing. However, the resulting distributions still show much higher imbalance and significant shape differences compared to the measured signal. This smearing cannot alone account for the magnitude of the rebalancing, confirming that the energy restored via low p_T constituents is correlated with the jet fragmentation.

In order to assess if the observed softening of the jet fragmentation is accompanied by a broadening of the jet profile, a measurement of the dijet imbalance with a resolution parameter of $R = 0.2$ was performed in an analogous fashion to the measurement described above. As shown in Fig. 3, narrowing the cone to $R = 0.2$ leads to significant differences between central Au + Au and embedded *pp* for jets with hard cores, with a *p* value of
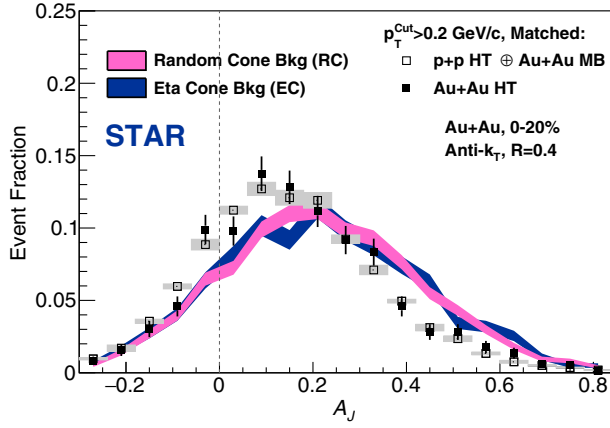
FIG. 2. A_J distributions for Au + Au data (filled symbols) and *pp* HT Au + Au MB (open symbols) for low constituent p_T^{Cut} dijets from Fig. 1 compared to A_J distributions calculated assuming the RC and EC null hypotheses, respectively, shown as colored bands; see the text for details. Stat. errors may be smaller than symbol size for *pp* HT Au + Au MB.

1×10^{-8} (1×10^{-9}–3×10^{-7}). Including soft constituents down to 0.2 GeV/c is no longer sufficient to restore the imbalance to the level of the *pp* reference. This continued disparity between the *pp* and Au + Au data is supported by a calculated *p* value of 7×10^{-8} (2×10^{-8}–4×10^{-7}). As a conservative test whether the different balancing behavior between $R = 0.2$ and $R = 0.4$ could be caused purely by smearing due to additional fluctuations, the matched $R = 0.2$ dijet pairs, i.e. including soft constituents, for both Au + Au HT and *pp* HT ⊕ Au + Au MB were embedded into rings with inner radius 0.2 and outer radius 0.4 selected randomly from 0%–20% MB Au + Au in an analogous
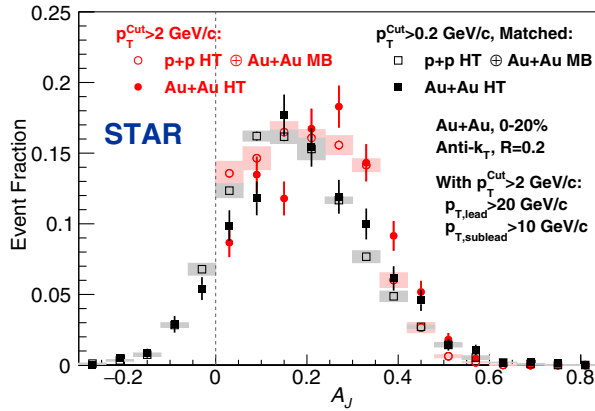

FIG. 3.   Repetition of the analysis shown in Fig. 1 with a smaller resolution parameter $R = 0.2$. Normalized A_J distributions for Au + Au HT data (filled symbols) and *pp* HT ⊕ Au + Au MB (open symbols). The red circles are for jets found using only constituents with $p_T^{Cut} > 2$ GeV/c and the black squares are for matched jets found using constituents with $p_T^{Cut} > 0.2$ GeV/c. Stat. errors may be smaller than symbol size for *pp* HT ⊕ Au + Au MB.

manner to the RC method above. Significant differences with a *p* value of 2×10^{-6} (1×10^{-4}–3×10^{-7}) remained in the A_J distribution that were not seen in true $R = 0.4$ jets.

In all descriptions of the QGP, energy redistribution via gluon bremsstrahlung is dependent on in-medium path length. Requiring high-p_T hadrons in the measured final state therefore imposes a significant bias toward production near the surface of the fireball, a paradigm known as surface bias. Previous STAR jet-hadron measurements are well captured by YAJEM-DE, a Monte Carlo model of in-medium shower evolution that predicts just such a surface bias for the same leading jet selection as used in this Letter [16,31].

The initial hard core dijet selection places hard hadron requirements on the recoil jet in addition to those on the leading jet. In the surface bias picture, they are therefore expected to display a pronounced preference toward almost tangential dijets, probes that graze the medium with a shorter but finite in-medium path length compared to the unbiased dijet selection at LHC energies [32]. Correlation measurements with two hard particles as jet proxies support the presence of such a tangential bias as well [33]. Our measurements of clearly modified jets whose "lost" energy can nevertheless be recovered within a comparatively narrow cone are qualitatively consistent with this picture.

The qualitative change in the dijet imbalance for smaller R jets as reported in this Letter is the first step towards enabling jet geometry engineering of jet production points which will allow control over the path lengths and interaction probabilities of jet quenching effects within the colored medium. In addition it would be very interesting to repeat this A_J study with "hard core" dijets at the LHC to see if a similar energy loss pattern is observed when similar jet pairs are selected. Comparison and combined analysis of these new RHIC results and current published LHC measurements will already enable new and enhanced constraints to be placed on the dynamics underlying modified fragmentation and energy dissipation in heavy-ion collisions.

In conclusion, we reported the first A_J measurement performed at $\sqrt{s_{NN}} = 200$ GeV. A selection of dijet pairs with hard cores is probed. For a resolution parameter of $R = 0.4$, a clear increase in dijet momentum imbalance is observed compared to a *pp* baseline when only constituents with $p_T^{Cut} > 2$ GeV/c are considered. When allowing softer constituents down to $p_T^{Cut} > 0.2$ GeV/c, the energy balance becomes the same within errors as the one measured in *pp* data. By contrast, repeating the same measurement with a smaller resolution parameter of $R = 0.2$ leads to significant remaining momentum imbalance even for jets with soft constituents. The results are the first indication that at RHIC energies it is possible to select a sample of reconstructed dijets that clearly lost energy via interactions with the medium but whose lost energy reemerges as soft constituents accompanied with a

small, but significant, broadening of the jet structure compared to *pp* fragmentation. The above observations are consistent with the qualitative expectations of pQCD-like radiative energy loss in the hot, dense medium created at RHIC.

---

[1] J. Adams *et al.* (STAR Collaboration), Nucl. Phys. **A757**, 102 (2005); K. Adcox *et al.* (PHENIX Collaboration), Nucl. Phys. **A757**, 184 (2005); I. Arsene *et al.* (BRAHMS Collaboration), Nucl. Phys. **A757**, 1 (2005); B. B. Back *et al.* (PHOBOS Collaboration), Nucl. Phys. **A757**, 28 (2005).

[2] B. Abelev *et al.* (STAR Collaboration), Phys. Rev. Lett. **99**, 142003 (2007).

[3] K. Adcox *et al.* (PHENIX Collaboration), Phys. Rev. Lett. **88**, 022301 (2001); I. Arsene *et al.* (BRAHMS Collaboration), Phys. Rev. Lett. **91**, 072305 (2003); J. Adams *et al.* (STAR Collaboration), Phys. Rev. Lett. **91**, 172302 (2003); B. B. Back *et al.* (PHOBOS Collaboration), Phys. Rev. Lett. **91**, 072302 (2003).

[4] M. Aggarwal *et al.* (STAR Collaboration), Phys. Rev. C **82**, 024912 (2010).

[5] M. Gyulassy and M. Plumer, Phys. Lett. B **243**, 432 (1990).

[6] A. Majumder and M. Van Leeuwen, Prog. Part. Nucl. Phys. **66**, 41 (2011).

[7] K. M. Burke, Buzzatti *et al.* (JET Collaboration), Phys. Rev. C **90**, 014909 (2014).

[8] G.-Y. Qin and X.-N. Wang, Int. J. Mod. Phys. E **24**, 1530014 (2015).

[9] M. Cacciari, G. P. Salam, and G. Soyez, Eur. Phys. J. C **72**, 1896 (2012).

[10] J. Adam *et al.* (ALICE Collaboration), Phys. Lett. B **746**, 1 (2015).

[11] S. Chatrchyan *et al.* (CMS Collaboration), Phys. Rev. C **84**, 024906 (2011).

[12] G. Aad *et al.* (ATLAS Collaboration), Phys. Lett. B **719**, 220 (2013).

[13] G. Aad *et al.* (ATLAS Collaboration), Phys. Rev. Lett. **105**, 252303 (2010).

[14] S. Chatrchyan *et al.* (CMS Collaboration), Phys. Lett. B **712**, 176 (2012).

[15] V. Khachatryan *et al.* (CMS Collaboration), J. High Energy Phys. 02 (2016) 156.

[16] L. Adamczyk *et al.* (STAR Collaboration), Phys. Rev. Lett. **112**, 122301 (2014).

[17] A. Adare *et al.* (PHENIX Collaboration), Phys. Rev. Lett. **111**, 032301 (2013).

[18] M. Anderson *et al.*, Nucl. Instrum. Methods Phys. Res., Sect. A **499**, 659 (2003).

[19] M. Beddo *et al.* (STAR Collaboration), Nucl. Instrum. Methods Phys. Res., Sect. A **499**, 725 (2003).

[20] L. Adamczyk *et al.* (STAR Collaboration), Phys. Rev. Lett. **115**, 092002 (2015).

[21] M. Cacciari, G. P. Salam, and G. Soyez, J. High Energy Phys. 04 (2008) 005.

[22] See Supplemental Material at http://link.aps.org/supplemental/10.1103/PhysRevLett.119.062301, which includes Refs. [23–29], for an evaluation of instrumental and heavy-ion background effects.

[23] T. Sjostrand, S. Mrenna, and P. Z. Skands, J. High Energy Phys. 05 (2006) 026.

[24] H. L. Lai, J. Huston, S. Kuhlmann, J. Morfin, F. I. Olness, J. F. Owens, J. Pumplin, and W. K. Tung (CTEQ Collaboration), Eur. Phys. J. C **12**, 375 (2000).

[25] R. Brun, F. Bruyant, M. Maire, A. C. McPherson, and P. Zanarini, Report No. CERN-DD-EE-84-1, 1987.

[26] B. I. Abelev *et al.* (STAR Collaboration), Phys. Rev. Lett. **100**, 232003 (2008).

[27] L. Adamczyk *et al.* (STAR Collaboration), arXiv:1702.01108.

[28] B. Abelev *et al.* (ALICE Collaboration), J. High Energy Phys. 03 (2012) 053.

[29] A. Ohlson, Ph.D. thesis, Yale University, 2013.

[30] I. M. Chakravarti, R. G. Laha, and J. Roy, *Handbook of Methods of Applied Statistics* (John Wiley and Sons, New York, 1967), Vol. 1, pp. 392–394.

[31] T. Renk, Phys. Rev. C **87**, 024905 (2013).

[32] T. Renk, Phys. Rev. C **85**, 064908 (2012).

[33] L. Adamczyk *et al.* (STAR Collaboration), Phys. Rev. C **87**, 044903 (2013).